

Cross Layer Multirate Adaptation Using Physical Capture

Jun Cheol Park*, Sneha Kumar Kasera* and Neal Patwari†

*School of Computing, University of Utah

Email: {jcpark, kasera}@cs.utah.edu

†Electrical and Computer Engineering, University of Utah

Email: npatwari@ece.utah.edu

Abstract—In this paper, to improve the performance of multihop wireless networks, we explore a cross layer multirate adaptation scheme (we call it CROMA) that uses the phenomenon of physical capture at the physical layer for effectively distinguishing losses due to collisions from those due to channel-error. We first estimate the number of packets dropped due to collisions, at each node by counting the number of packets that are not successfully retrieved by physical capture. Next, using a simple algorithm, we assign this collision loss to neighboring sources of packets that might have generated the colliding packets. Using extensive *ns-2* simulations, we show that our multirate adaptation scheme consistently outperforms the existing schemes.

I. INTRODUCTION

Multirate adaptation capability for dynamically adapting to diverse channel conditions is critical in improving the performance of IEEE 802.11-based multihop wireless networks although it is left unspecified in the IEEE 802.11 standard [1], [2]. There is a fundamental trade-off between a selected data rate and its associated packet delivery ratio. In general, a higher data rate is associated with a lower packet delivery ratio. The key idea of multirate adaptation schemes is to find a data rate that can maximize the product of the selected data rate and its associated packet delivery ratio. Although this trade-off is tied to instantaneous channel conditions of wireless links at the physical layer, the medium access control (MAC) layer determines the data rate that should be used for each transmission. Developing an effective multirate adaptation scheme at the MAC layer is challenging mainly due to lack of the accurate assessment of the instantaneous channel conditions at the physical layer.

In recent years, a number of multirate adaptation schemes (ARF [3], AARF [15], SampleRate [4], HRC [9], CARA [10], RRAA [17]) have been proposed. In these schemes, a *packet loss on a wireless link* is used to estimate channel conditions. A packet loss event is considered to be an indication of the data rate at which the packet is transmitted being too high for the given instantaneous channel condition, and used to downgrade the rate of transmission. However, in multihop wireless networks, not all packet losses are due to poor channel conditions. Packets can also be lost due to collisions when packet transmissions overlap. When a packet is lost due to collisions while channel conditions on a wireless link are good, a node must not downgrade its data rate. Rather, it must take contention avoidance actions to prevent future collisions. In

contrast, when a packet is lost due to channel-error, a data rate downgrade becomes necessary to cut down packet loss and prevent wastage of the channel capacity. We have found that [11] the existing multirate adaptation schemes do not effectively differentiate the causes of packet loss in multihop wireless networks, and hence perform poorly.

In this paper, to improve the performance of multihop wireless networks, we explore a cross layer multirate adaptation scheme (we call it CROMA) that uses the phenomenon of physical capture at the physical layer for effectively distinguishing losses due to collisions from those due to channel-error. Nodes in this scheme exchange collision loss information obtained by the physical capture to extract channel-error loss from the total measured loss. Physical capture gives a wireless node the capability to retrieve the packet with the stronger signal even when it receives two packets that overlap in time. We first estimate the number of packets dropped due to collisions, at each node by counting the number of packets that are not successfully retrieved by physical capture. Next, using a simple, yet effective algorithm, we assign this collision loss to neighboring sources of packets that might have generated the colliding packets. Our algorithm assigns collision loss to a neighboring node in proportion to the number of transmissions sent by it.

Each node uses a special control packet to send out the number of packets it transmits to neighboring receivers. The computed collision loss, that a node measures while performing the task of a receiver, as well as the identity of the sources to which this collision loss is proportionately assigned, is also included in the control packet. Once the collision loss is available at a source node, it subtracts this collision loss from the total measured loss to accurately determine the loss due to channel-error only. This measure of loss due to channel-error only is then used for data rate control. Like the existing schemes [9], [17], we use a threshold-based decision scheme where the data rate is downgraded or upgraded when the measured packet loss is greater than or less than certain thresholds, respectively. However, we use accurate channel-error loss that is adjusted by collision loss obtained by the physical capture.

We use extensive *ns-2* [16] simulations in order to evaluate our CROMA scheme in diverse channel conditions. Specifically, we add the IEEE 802.11a PHY that uses orthogonal

frequency-division multiplexing (OFDM) for providing high data rates in $ns-2$. We further enhance $ns-2$ so that physical capture can be achieved as long as the conditions for a successful physical capture are met. The empirical results of physical capture obtained from [14] are used as the conditions for a successful physical capture in $ns-2$. Our simulation results show that our multirate adaptation scheme consistently outperforms the existing schemes.

The rest of this paper is organized as follows. In the next section, we summarize the relevant existing work. In section III, we describe our CROMA scheme in detail. We provide our simulation model to evaluate our CROMA scheme in diverse channel conditions in Section IV and compare the performance of our schemes with the other existing work in Section V. We conclude our work in Section VI.

II. RELATED WORK

There is a significant amount of work on rate control in IEEE 802.11 networks [3]–[5], [9], [10], [17], [18]. We provide an extensive survey in [11]. Our work differs from the existing work in our use of physical capture for multirate adaptation in multihop networks.

In this paper, we compare our work with a very recent multirate adaptation scheme, Robust Rate Adaptation Algorithm (RRAA) [17]. RRAA uses a short term packet loss measurement scheme at a wireless node to adaptively determine the best data rate (that is called RRAA-BASIC). It also makes an adaptive use of RTS/CTS to avoid collisions when there are hidden nodes in the wireless network (so-called RRAA-ARTS). Our work differs from RRAA in the following significant ways. First, our work explicitly measures collision loss (using physical capture) unlike RRAA, which depends on RTS/CTS to reduce collisions. Second, RRAA has been evaluated only for infrastructure networks. Our evaluation is much more general. We compare our scheme CROMA to RRAA-BASIC and RRAA-ARTS because these outperform the other existing schemes such as ARF [3], AARF [15], and SampleRate [4], as shown in [17]. We believe that our work is the first one to thoroughly investigate multirate adaptation schemes in multihop wireless networks using physical capture.

Recent work on analog coding [12] proposes to aggressively exploit collisions rather than avoid them. A new collision resolution approach called ZigZag, has been proposed recently [7]. Although both of the above approaches [7], [12] on collision resolution provide efficient ways to handle collisions in simple collision scenarios, they have not been investigated and evaluated in multihop ad hoc networks.

III. CROMA SCHEME

In this section, we present our cross layer multirate adaptation scheme (CROMA) to improve the performance of multihop wireless networks. Our scheme distinguishes packet losses due to collisions from those due to channel-error by using *physical capture* and a cooperative exchange of loss information between senders and receivers in the wireless

TABLE I
REQUIRED SNR (DB) TO RETRIEVE STRONGER PACKETS

Data Rate of Stronger Packet	Required SNR Difference
6 Mbps	3 dB
9 Mbps	3 dB
12 Mbps	3 dB
18 Mbps	6 dB
24 Mbps	10 dB
36 Mbps	16 dB
48 Mbps	24 dB
54 Mbps	24 dB

network. The collision loss is subtracted from the total loss to accurately determine the channel-error loss.

A. Physical Capture

With physical capture, a wireless card is able to retrieve the packet with the stronger signal even when it receives two packets that overlap in time under the following conditions: (i) The difference in the SNR value of the stronger packet and the weaker packet should exceed a threshold, and (ii) the two packets should be separated at least with a minimum arrival time gap (e.g., $16 \mu s$ ¹). The stronger packet can be retrieved even if it arrives later (called the “stronger-last collision”). This retrieval attempt in the stronger-last collision case is also called *message in message* (MIM) mode transition where a node transits its current receiving process to a new packet with a higher SNR [14]. To support the MIM mode transition, a wireless card has a simple mechanism to detect a higher SNR of a new packet while receiving its first packet. Note that physical capture is still effective without invoking the MIM mode transition when a first packet has a higher SNR than a second packet. A required SNR difference to retrieve stronger packets depends on the data rate at which the stronger packets are transmitted, regardless of the data rates of weaker packets, as observed by Lee et al. [14]. Table I (extracted from the empirical results in [14]) shows the different SNR values between two overlapping packets to retrieve the stronger packet is higher at higher data rate of the stronger packet. For instance, for a stronger packet transmitted at 6 Mbps, the required SNR difference is 3 dB whereas at least 10 dB of SNR difference is required to retrieve the stronger packet when transmitted at 24 Mbps. When the SNR difference is not enough to retrieve the stronger packet for a specific data rate, neither of the overlapping packets can be decoded correctly. Physical capture capability already exists in some well-known IEEE 802.11 compliant wireless cards [6], [8].

Our key idea is to detect the transmission overlappings as a byproduct of the physical capture process, and use the count of these overlappings to estimate collisions. However, there are two critical challenges that we must address in applying physical capture for estimating collision loss. First, it is not always possible to count *every* collision even with physical capture. When a weaker packet arrives later than a stronger packet, the stronger packet continues to be proceeded

¹The threshold and the minimum arrival time gap depend upon the physical layer modulation technique.

to be decoded without knowing that there is a transmission overlapping, and the weaker packet ceases to be retrieved resulting in being dropped due to collision. This is because the MIM mode transition is invoked *only* when the node detects a higher SNR of a new packet while receiving its first packet. The second challenge is how to find which node has transmitted the packets that are dropped due to collisions. When a packet cannot be retrieved due to a collision, the source MAC address of the packet cannot be found either. We provide our solutions to address these two challenges in the next two subsections.

B. Estimating Number of Collisions

We use a simple method for counting the total number of dropped packets at a receiver due to collisions as well as the total number of packets that are transmitted by all neighboring nodes. The main idea of our method is to categorize the events of collisions into two cases, depending on whether or not a stronger packet is successfully retrieved during physical capture. Case (i): When a stronger packet that arrives later than a weaker packet, thereby invoking a MIM mode transition, is successfully retrieved, we consider the number of dropped packets associated with this event as two. This is because it is highly likely for the stronger packet to arrive earlier than the weaker packet with equal probability, which is *undetectable* by physical capture. In this event of retrieval of the stronger packet, the number of associated retrieved packets is also doubled up to approximate the total number of retrieved packets during collisions for the associated sender node. Case (ii): When a stronger packet which arrives later than a weaker packet, thereby invoking a MIM mode transition, fails to be retrieved (i.e., the two packets fail to be retrieved due to collision), we also consider the number of dropped packets associated with this event as four rather than two. This is because the both packets would also be dropped when the stronger packet arrives earlier without invoking a MIM mode transition, which again is *undetectable*. Thus, any detectable packet drop during physical capture is again doubled up to approximate the total number of dropped packets due to collisions.

More formally, let C_i denote the number of packets, from sender i ($i \in$ all neighboring sender nodes, n), that a receiver node fails to receive due to collisions over the last Δ time units (e.g., one second). What the receiver node needs to know are all C_i s, corresponding to all of its neighbor nodes, for a given total number of dropped packets due to collisions.

Table II shows variables their descriptions that we use for finding the C_i s in this section. All variables in the table are measured or derived over Δ time units. D_i is the total number of the packets transmitted by a sender node i , that is successfully retrieved after a MIM mode transition is invoked. This notation of D_i can also be interpreted as the total number of dropped packets while these packets sent by node i are retrieved. B is the number of times both of the two overlapping packets are dropped due to collisions even after the MIM mode transition is invoked and the physical capture process

TABLE II
NOTATIONS

Measured Variables	Descriptions
n	The number of neighboring sender nodes.
D_i	The number of dropped packets sent by other nodes while packets sent by node i are successfully retrieved.
B	The number of times both of the overlapping packets fail to be retrieved due to collisions, even after a MIM mode is invoked.
E	The number of receiving packets that do not incur a MIM mode transition
T_i	The number of packets transmitted by node i
Derived Variables	Descriptions
I	The total number of packets dropped due to collisions equal to $4B + \sum_{i=1}^n 2D_i$
R_i	$T_i / (\sum_{k=1}^n T_k)$
$R'_i(j)$	$T_i / (\sum_{k=1, k \neq j}^n T_k)$
N	The total number of arriving packets including all colliding packets
C_i	The total number of packets sent by node i , that are dropped due to collisions

tries to retrieve the stronger packet. Let T_i denote the number of packets, transmitted by node i (this information will be periodically delivered to the receiver from the sender node i , as explained in Section III-C).

Now, the total number of packets dropped due to collisions, I , can be approximated by $4B + \sum 2D_i$, as we described above. In order to estimate each C_i from I , we first assign $4B$ in proportion to the number of packets sent by node i . That is, we assign $4B \times R_i$ to C_i , where R_i is the ratio of T_i to $\sum_{k=1}^n T_k$. Next, we assign $\sum_{j=1, j \neq i}^n 2D_j$ to C_i , again in proportion to the number of packets sent by node i . However, note that in this proportionate assignment of $2D_j$, we use $R'_i(j)$ rather than R_i because the node j is not involved in $2D_j$, where $R'_i(j)$ is the ratio of T_i to $\sum_{k=1, k \neq j}^n T_k$. Therefore,

$$C_i = 4B \times R_i + \sum_{j=1, j \neq i}^n (2D_j \times R'_i(j)) \quad (1)$$

We have showed in [11] that this assignment of collisions is complete in the sense that the total sum of C_i s is equal to I (the property of mutually disjoint in the assignment is trivial by the definition of C_i).

C. Special Control Packet

In order for a node i to inform nearby sender nodes about collision loss and the number of transmitted packets, our scheme periodically broadcasts a special control packet with a random jitter. The random jitter is useful in avoiding possible collisions with other transmissions when there are multiple competing nodes in ad hoc networks. This new control packet consists of an array of elements, one element for each sender. Each element is of 9-bytes comprising three fields: a 6-byte

MAC address of the sender node, the corresponding 1-byte collision loss (which ranges from 0% to 100%), and a 2-byte number of transmitted packets. For instance, when the number of elements in a control packet is eight, the packet size is still less than 100 bytes. This small control packet is always transmitted at 6 Mbps data rate like RTS/CTS control packets. We find the overhead of our control packet to be negligible in our simulations (see our evaluation Section V).

D. Estimating Number of Arriving Packets

In order to estimate collision loss, we still need to know how many packets arrive at a receiver including packets that collide over the time Δ . One may simply use the sum of all T_k s obtained by all neighboring nodes to find the number of packets arriving at the receiver. However, this may be inaccurate due to possible delays in receiving the packets that include these T_k s. That is, in the T_k values sent by a sender to the receiver might not arrive in time. In order to robustly estimate the total number of arriving packets, we use a direct measure of all arriving packets at a receiver node.

Let S denote the number of times that a single packet, successfully decoded or not, is being received without any transmission overlapping. Then, the total number of arriving packets, N , can be simply expressed by $S + \sum_{i=1}^n 4D_i + 4B$. Note that D_i is multiplied by four (rather than two) because we also need to count the total number of arriving packets including packets that are not retrieved due to weaker signals. The problem is, however, that S cannot be separately measured from other cases where there is a transmission overlapping that does not incur a MIM mode transition.

To resolve this problem, we use an approximate method to estimate N . Now, let E denote the total number of times that a node is receiving a packet, successfully decoded or not, without invoking a MIM mode transition in the middle of the receiving process. E can be easily measured because a sender node can simply count the number of times that its receiving process does not invoke a MIM mode transition. However, this number E includes all the following three cases: (i) A single packet, successfully decoded or not, is being received without any transmission overlapping, (ii) With a transmission overlapping, a packet is being received and successfully decoded during physical capture, and (iii) With a transmission overlapping, a packet is being received, but fails to be retrieved even with physical capture. Note that the case (ii) is reminiscent of the notation of D_i and so the case (iii) is of the notation of B except for the order of stronger and weaker packets, as defined in Section III-B. In fact, E can be expressed by $S + \sum_{i=1}^n D_i + B$. Therefore, we can approximate $N (= S + \sum_{i=1}^n 4D_i + 4B)$ using E as follows.

$$N \simeq E + \sum_{i=1}^n 3D_i + 3B \quad (2)$$

Finally, for each sender i at a receiver node r , the collision loss, denoted by $c(i, r)$, can be approximated by C_i/N . $c(i, r)$ is computed and updated periodically every τ time units (e.g.,

every 500 milliseconds, in accordance with the frequency of the special control packet broadcast), by measuring C_i and N over the last time Δ (e.g., every second). The node r periodically broadcasts, with a random jitter, a special small control packet that includes the collision loss $c(i, r)$ along with the corresponding sender identity r to all the senders from which it receives packets. (explained in detail in the next section). Then, each sender node that receives this control packet is able to find the loss of its packets due to collisions at node r .

E. Channel-Error Calculation

Packet losses at a sender node are measured by calculating the difference in the number of packets sent and the number of acknowledgments received. For a given measured packet loss, each node needs to extract the actual channel-error loss by removing packet losses due to collisions. We provide a simple way to estimate the channel-error loss at a sender node using the collision loss received from the receiver nodes.

Let $l(i, r)$ denote a measured packet loss of a wireless link between a sender node i and a receiver node r in the time period Δ . Note that $l(i, r)$ includes packet losses due to both collisions and channel-error. We want to determine the channel-error loss, $p(i, r)$, between the sender node i and the receiver node r , based on $c(i, r)$ ($=C_i/N$ at a receiver r) and $l(i, r)$. If there is a collision drop when a packet is transmitted to node r from node i , the packet will be discarded regardless of channel-error on the link. If there is no collision, the packet will be lost only due to channel-error on the link. Therefore, assuming that collision and channel-error drop events are independent of each other, the measured packet loss $l(i, r)$ at the sender node i can be expressed as follows.

$$\begin{aligned} l(i, r) &= c(i, r) + (1 - c(i, r)) \times p(i, r) \\ \iff p(i, r) &= \frac{l(i, r) - c(i, r)}{1 - c(i, r)} \end{aligned} \quad (3)$$

Thus, a node uses Eq. (3) to calculate $p(i, r)$ using $c(i, r)$ and $l(i, r)$. Like $c(i, r)$, $l(i, r)$ is computed every τ time units.

F. Rate Decision Algorithm

RRAA [17] provides a way to calculate an opportunistic rate increase threshold (ORI) and a maximum tolerable loss threshold (MTL) for each data rate where a node upgrades or downgrades its current data rate whenever the packet loss is less than ORI or greater than MTL, respectively. For the IEEE 802.11a PHY data rates, all ORI values (Table 3 in [17]) range between 5% and 20% and MTL values reside between 20% and 40%. We use the original values of MTL's and ORI's from RRAA. However, we use our channel-error loss $p(i, r)$ that is extracted from measured packet loss $l(i, r)$ by collision loss $c(i, r)$ in determining the best data rate. Our rate decision algorithm is described in Fig. 1. When $p(i, r)$ is too high compared to an ORI(R) with the current data rate R, then the algorithm downgrades R. When $p(i, r)$ is lower than an MTL(R) with the current data rate R, the algorithm upgrades R.

R : the current selected data rate at PHY.
 $l(i, r)$: the measured packet loss between node i and r for the given R .
 $c(i, r)$: the measured collision loss between node i and r .
 1: $p(i, r) = \frac{l(i, r) - c(i, r)}{1 - c(i, r)}$
 2: if $(p(i, r) > MTL(R))$ then
 3: Downgrade to $R-1$
 4: else if $(p(i, r) < ORI(R))$ {
 5: else Upgrade to $R+1$ }

Fig. 1. CROMA rate decision algorithm

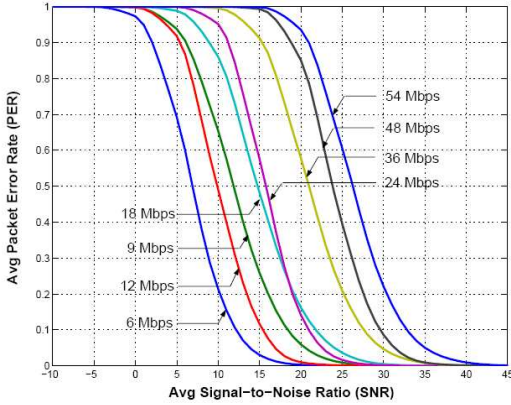


Fig. 2. Packet error rate vs. SNR value (dB) for each data rate in IEEE 802.11a on the ESTI channel model A. Application payload size is 1464 bytes. Actual size at PHY is 1528 bytes including TCP (20) and IP (20) headers, and the MAC (24) header.

IV. SIMULATION MODEL

In this section, we describe our simulation model for evaluating our CROMA scheme and comparing its performance with the RRAA scheme.

A. IEEE 802.11a PHY and MAC

We simulate the IEEE 802.11a PHY that is based on OFDM with convolutional coding by implementing OFDM features in the network simulator *ns-2* [16]. We validate our 802.11a implementation in *ns-2* by comparing the throughput of an 802.11a link for each data rate with that of a channel-error free wireless link in the Emulab wireless testbed. The details of our OFDM implementation are described in [11]. As observed in [13], [14], the physical capture available in *ns-2* is only partially correct because it does not implement the MIM mode transition (i.e., the “stronger-last collision” resolution). We modify *ns-2* so that physical capture can be achieved regardless of whether the stronger packet arrives before or after the weaker packet as long as the conditions for a successful physical capture are met. We use a threshold of 3 dB for invoking physical capture and $16 \mu s$ as the minimum arrival time gap of the two packets (i.e., preamble detection time in IEEE 802.11a).

B. Packet Error – Average SNR Profile

To create error-prone wireless links in *ns-2* [16] simulations, we use the ETSI (European Telecommunications

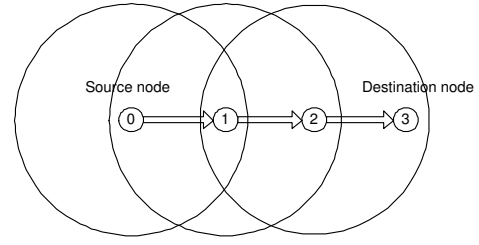


Fig. 3. A 3-hop ad hoc path in IEEE 802.11a. The circle around a node represents its transmission and carrier sensing range.

Standards Institute) channel model A for packet error rate-average SNR profile from [19]. Fig. 2, borrowed from [19], shows this profile for different data rates. The ETSI channel A is a typical indoor environment with a root mean square (RMS) delay spread of 50 nanoseconds, without line-of-sight (LOS). We use this profile to create diverse channel conditions in our simulations.

V. EVALUATION

In this section, we evaluate our scheme CROMA using extensive *ns-2* simulations, by comparing our scheme with a very recent multirate adaptation scheme, Robust Rate Adaptation Algorithm (RRAA) [17]. We use a static ad hoc routing to avoid any possible effect of routing protocols. We first analyze the performances on a 3-hop ad hoc path with a single TCP or UDP flow under diverse channel conditions. Next, we also evaluate CROMA in scenarios where there exist multiple senders/receivers in order to observe how well CROMA differentiates multiple senders/receivers in estimating collision loss. In all experiments, we use the PHY layer parameters as described in section IV-A and the ESTI channel model A, described in section IV-B with the packet size of 1464 bytes at the application layer. We also use $\Delta = 1$ second as the sliding window size.² We periodically broadcast special control packets that include both collision loss and the number of transmitted packets per destination node every τ time units. We use $\tau = 500$ milliseconds. We find that at this rate, the control packets add negligible overhead while providing enough agility to share measured information with neighboring nodes.

A. Single Ad Hoc Paths

It has been shown in [11] that an ad hoc path whose hop number is greater or equal to three³ in IEEE 802.11a may experience considerable collisions that perturb measured loss in the existing multirate adaptation schemes. In order to observe how well our scheme CROMA performs in such an environment, we use the IEEE 802.11a-based 3-hop ad hoc path, as shown in Fig. 3. The circle around each node represents its transmission range and its physical carrier sensing range. For longer ad hoc paths, we expect to obtain essentially similar results. We assume that every link on the 3-hop ad

²We find that the sliding window size of 1–2 seconds effectively deals with changes in channel conditions.

³This number would be four in 802.11b.

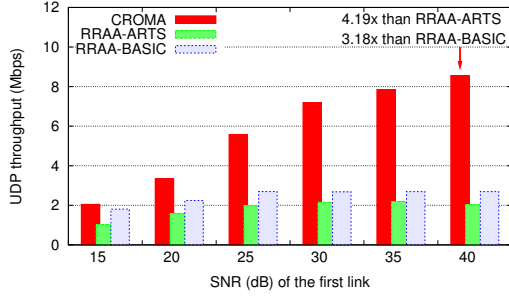


Fig. 4. INC case: UDP throughput for RRAA-BASIC, RRAA-ARTS and CROMA.

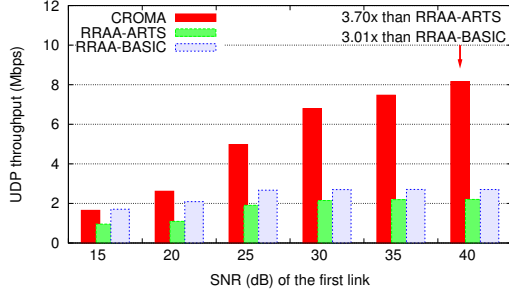


Fig. 5. IDC case: UDP throughput for RRAA-BASIC, RRAA-ARTS and CROMA.

hoc path has a fixed (but not necessarily the same) average SNR value. In order to conduct various channel conditions of wireless links on a 3-hop ad hoc path, we use different patterns of SNR values on the three links, Link 1, Link 2, and Link 3. Let Q_i denote the average SNR value of the Link i . There are four different cases on their relationship according to the values of Q_i 's: (i) $Q_1 \leq Q_2 \leq Q_3$ (INC: increasing), (ii) $Q_1 \leq Q_2 \geq Q_3$ (IDC: increasing and decreasing), (iii) $Q_1 \geq Q_2 \geq Q_3$ (DEC: decreasing), and (iv) $Q_1 \geq Q_2 \leq Q_3$ (DIC: decreasing and increasing). We use 3 dB as the threshold for invoking the MIM mode transition. As a result, when SNR differences on adjacent links are less than 3 dB, our scheme that uses physical capture is not able to detect any transmission overlappings. However, in practice, it is very likely that adjacent links along ad hoc paths have SNR differences more than 3 dB. In cases where the SNR differences are less than 3 dB, we find that the performance of CROMA is at least 97% of that of the existing RRAA scheme, implying that even when the conditions are not congenial for its operation, our scheme performs at par with RRAA.

To evaluate how well our scheme performs in all other environment, we use 3 dB as a minimum gap of SNR values between adjacent links. We first analyze UDP performance in all the four cases INC, IDC, DEC, and DIC, followed by TCP performance in the same cases.

B. UDP Performance

Fig. 4, 5, 6, and 7 show the comparisons of UDP performance, for the four patterns of INC, IDC, DEC, and DIC, respectively, under the three schemes, RRAA-BASIC, RRAA-ARTS, and our CROMA scheme, over 90 seconds. The x-axis represents the SNR value of the first link on the 3-hop ad hoc path. According to each SNR change pattern, the SNR values

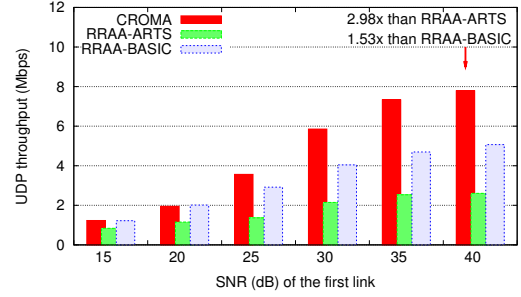


Fig. 6. DEC case: UDP throughput for RRAA-BASIC, RRAA-ARTS and CROMA.

of the subsequent links (i.e., Link 2 and Link 3) are smaller or larger than the first link's SNR value by a fixed gap. In all experiments, we use 3 dB for increasing or decreasing the SNR value of subsequent links. For instance, for the INC scenario, when the SNR value of the first link is 20 dB, the SNR values of Link 2 and 3 are 23 dB and 26 dB, respectively. Likewise, for the IDC scenario, the SNR values of the two subsequent links are 23 dB and 20 dB. For other values of minimal SNR gap between adjacent links, we find essentially similar results as long as the SNR gap on adjacent links is greater than or equal to 3 dB.

Consider the two cases of INC and IDC, as shown in Fig. 4 and 5. For all different values of SNR, CROMA achieves up to 4.19x and 3.18x higher UDP performance in comparison to RRAA-ARTS and RRAA-BASIC, respectively. The common property of the both cases is that the second link has better channel conditions than the first link. It means that, when packets collide at Node 1, packets transmitted by Node 2 may be able to be retrieved, resulting in the phenomenon that Node 0 may experience relatively more packet losses due to collisions. In these INC and IDC cases, RRAA-BASIC always selects the lowest data rate of 6 Mbps for the first link on the 3-hop ad hoc path regardless of the given channel conditions because it does not differentiate the causes of packet loss. As a result, even when the channel condition is excellent (e.g., for the 40 dB case), the whole performance of the 3-hop ad hoc path in RRAA-BASIC is restricted to the bottleneck link (the first link) although, for the other two links, a 54 Mbps data rate is selected by RRAA-BASIC. For inferior channel conditions (SNR < 25 dB), the performance gain by CROMA compared to RRAA-BASIC, although still better, is marginal. This is because the chosen suitable data rates are close to 6 Mbps which is what RRAA-BASIC selects as well. However, for superior channel conditions (SNR \geq 25 dB), the performance gain by CROMA is more than 2x.

Interestingly, the performance of RRAA-ARTS is less than that of RRAA-BASIC for all cases. RRAA-ARTS also uses 6 Mbps for the first link because the adaptive use of RTS/CTS is not effective in finding suitable data rates with collisions. The use of RTS/CTS in RRAA-ARTS simply adds more overhead, but does not help.

Now, consider the other two cases of DEC and DIC where the SNR value of the second link is greater than that of the first link, as shown in Fig. 6 and 7. The common property of the

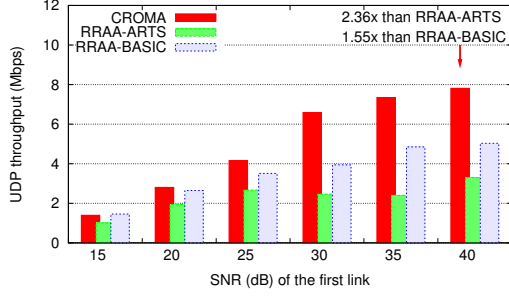


Fig. 7. DIC case: UDP throughput for RRAA-BASIC, RRAA-ARTS and CROMA.

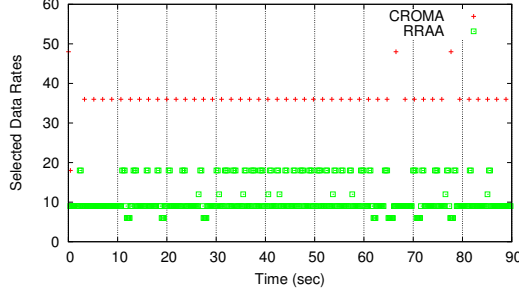


Fig. 8. DEC case: Comparison of Selected Data Rates in RRAA-BASIC and CROMA.

both cases is that, when packets collide at Node 1, packets sent by Node 0 may be able to be retrieved, resulting in the situation that Node 0 may not experience packet losses due to collision. When Node 0 does not experience many packet losses due to collisions, the measured packet loss by Node 0 is close to the channel-error in Link 1. RRAA selects the right data rates, as expected. As a result, for inferior channel conditions ($\text{SNR} < 25$ dB), the performance of CROMA is close to that of RRAA. However, for superior channel conditions ($\text{SNR} \geq 25$ dB), the performance gain by CROMA becomes up to 1.5x. This is because, even with the help of physical capture, when selected data rates are higher, colliding packets cannot be retrieved. When packets are lost even with physical capture, RRAA selects lower data rates because it considers these packet losses to be due to channel-error. Note that higher data rates require higher SNR gaps, as shown in Table I.

We now scrutinize the internal behaviors of each scheme for the DEC case. Fig. 8 shows the data rates selected by CROMA and RRAA at Node 0 when the SNR value of the first link is 30 dB for the DEC case. The data rates determined by RRAA fluctuate from 9 Mbps through 18 Mbps while the data rates chosen by CROMA mostly stay at 36 Mbps. The main reason of such fluctuation in RRAA is that the number of packets retrieved by physical capture changes according to the selected data rates. When lower data rates (e.g., 9 Mbps) are used by RRAA, colliding packets sent by Node 0 can be retrieved, causing reduction in the measured packet loss at Node 0. As a result, Node 0 upgrades its data rate and experiences higher packet loss caused by failures to retrieve packets at the upgraded data rate. When Node 0 starts experiencing higher packet loss mainly due to collisions, it downgrades its data rate. Node 0's data rates fluctuate due to its incapability to differentiate the cause of packet loss. Therefore, RRAA selects

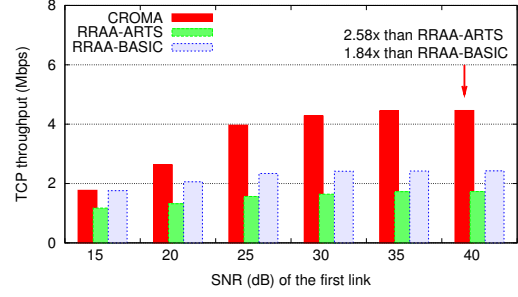


Fig. 9. INC case: TCP throughput for RRAA-BASIC, RRAA-ARTS and CROMA.

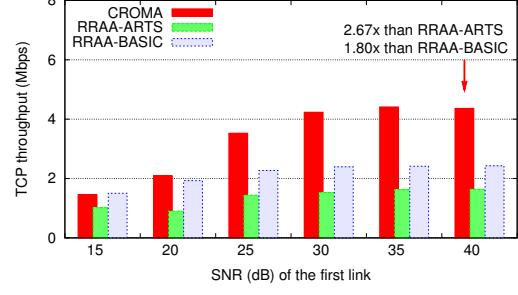


Fig. 10. IDC case: TCP throughput for RRAA-BASIC, RRAA-ARTS and CROMA.

data rates that are much lower than the most suitable data rates.

C. TCP Performance

Fig. 9, 10, 11, and 12 show the comparisons of TCP performance, for INC, IDC, DEC, and DIC, respectively, under the three schemes, RRAA-BASIC, RRAA-ARTS, and our CROMA scheme, over 90 seconds. The x-axis represents the SNR of the first link, and the y-axis represents the TCP throughput. Similar to the UDP performance, CROMA significantly achieves up to 2.67x and 1.84x higher TCP performance in comparison to RRAA-ARTS and RRAA-BASIC, respectively, for the INC and IDC cases. Compared to the UDP performance in Section V-B, the actual performance gain by CROMA is reduced from around 3x–4x to 1.8x–2.7x for the INC and IDC cases. The main reason for the reduced performance gain is that the TCP performance itself on a 3-hop ad hoc path is considerably reduced due to the overhead of TCP congestion control, resulting in the reduced gap between CROMA and RRAA. However, CROMA still significantly outperforms both RRAA-ARTS and RRAA-BASIC in the INC and IDC cases.

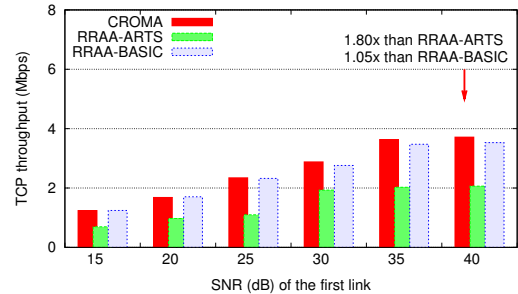


Fig. 11. DEC case: TCP throughput for RRAA-BASIC, RRAA-ARTS and CROMA.

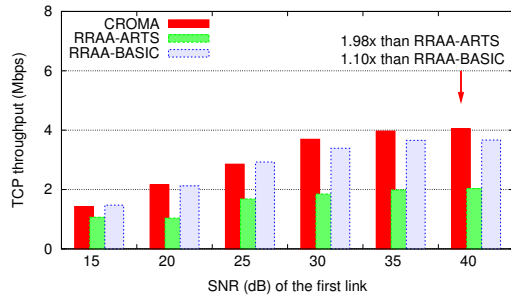


Fig. 12. DIC case: TCP throughput for RRAA-BASIC, RRAA-ARTS and CROMA.

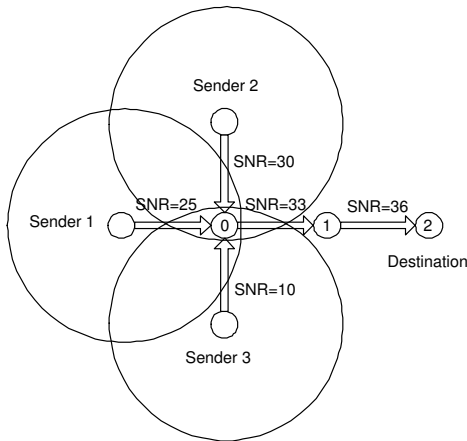


Fig. 13. Three Concurrent Senders in IEEE 802.11a. The circle around a node represents its transmission and carrier sensing range.

For the other two cases, DEC and DIC, Fig. 11 and 12 show the TCP performance. Although the performance of CROMA in the DEC case becomes close to that of RRAA-BASIC, the performance of CROMA in the DIC case is slightly better than that of RRAA-BASIC. As before, due to the overhead of TCP congestion control, the actual performance gain by CROMA is reduced, compared to the UDP scenarios.

D. Three Concurrent Senders

In order to evaluate how well CROMA operates with concurrent senders, we use the topology shown in Fig. 13 where three concurrent senders share an ad hoc path (except for their first link) toward a destination. Each sender in this topology is outside the carrier-sense range of other senders, and hence is hidden for the other senders. To evaluate how effectively CROMA adapts to diverse channel conditions, we

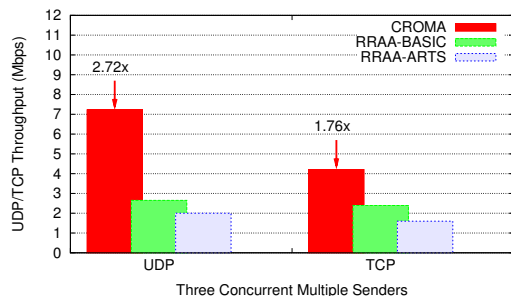


Fig. 14. Three Concurrent Senders: UDP/TCP throughput for CROMA, RRAA-BASIC, and RRAA-ARTS.

choose different SNR values for each sender's link. We also choose the remaining two links that have higher SNR values than any sender's link, as shown in Fig. 13. Fig. 14 shows the comparisons of the total throughput of UDP and TCP flows of the three schemes, RRAA-BASIC, RRAA-ARTS, and CROMA, over 90 seconds. We find that CROMA achieves up to 2.72x and 1.76x higher throughput in comparison to the RRAA-BASIC for UDP and TCP, respectively.

VI. CONCLUSION

We proposed a cross layer multirate adaptation scheme (CROMA) to improve the performance of multihop wireless networks. Our scheme effectively distinguished losses due to collisions from those due to channel-error in a multihop wireless network using physical capture. We developed a simple algorithm that assigns collision loss to neighboring sources of packets in proportion to the number of transmissions sent by them. Using extensive *ns-2* [16] simulations, we find that the use of physical capture significantly improves multirate adaptation thereby significantly improving TCP and UDP throughput in multihop wireless networks as well.

REFERENCES

- [1] IEEE Std 802.11a, Supplement to Part 11: Wireless LAN Medium Access Control (MAC) and Physical Layer (PHY) Specifications: High-speed Physical Layer in the 5 GHz Band, 1999.
- [2] IEEE Std 802.11b, Supplement to Part 11: Wireless LAN Medium Access Control (MAC) and Physical Layer (PHY) Specifications: Higher Speed Physical Layer Extension in the 2.4 GHz Band, 1999.
- [3] Ad Kamerman et al. WaveLAN-II: a High-Performance Wireless LAN for the Unlicensed Band. In *Bell Lab Tech Journal*, 1997.
- [4] J. C. Bicket. Bit-rate Selection in Wireless Networks, Master Thesis, MIT, 2005.
- [5] Charles Reis et al. Measurement Based Models of Delivery and Interference in Static Wireless Networks. In *ACM SIGCOMM*, 2006.
- [6] S. Ganu, K. Ramachandran, M. Gruteser, I. Seskar, and J. Deng. Methods for Restoring MAC Layer Fairness in IEEE 802.11 Networks with Physical Layer Capture. In *ACM REALMAN*, 2006.
- [7] S. Gollakota and D. Katabi. ZigZag Decoding: Combating Hidden Terminals in Wireless Networks. In *ACM SIGCOMM*, 2008.
- [8] Intersil Co. PRISM Driver Programmers Manual, July 2003 RM025.3.
- [9] Ivaylo Haratcherev et al. Hybrid Rate Control for IEEE 802.11. In *ACM MobiWac*, 2004.
- [10] Jongseok Kim et al. CARA: Collision-Aware Rate Adaptation for IEEE 802.11 WLANs. In *IEEE INFOCOM*, 2006.
- [11] Jun Cheol Park, "Channel-Error and Collision Aware, Secure Multihop Ad hoc Wireless Networks," Ph.D. dissertation, School of Computing, University of Utah 2008.
- [12] S. Katti, S. Gollakota, and D. Katabi. Embracing Wireless Interference: Analog Network Coding. In *ACM SIGCOMM*, 2007.
- [13] A. Kochut, A. Vasani, A. U. Shankar, and A. Agrawala. Sniffing out the Correct Physical Layer Capture Model in 802.11b. In *IEEE ICNP*, 2004.
- [14] J. Lee, W. Kim, S.-J. Lee, D. Jo, J. Ryu, T. Kwon, and Y. Choi. An Experimental Study On the Capture Effect in 802.11a Networks. In *ACM WINTeCH*, 2007.
- [15] Mathieu Lacage et al. IEEE 802.11 Rate Adaptation: A Practical Approach. In *ACM MSWiM*, 2004.
- [16] *Ns-2 simulator*.
- [17] Starsky H.Y. Wong et al. Robust Rate Adaptation for 802.11 Wireless Networks. In *ACM MOBICOM*, 2006.
- [18] Tamer Nadeem et al. IEEE 802.11 DCF Enhancements for Noisy Environments. In *IEEE PIMRC*, 2004.
- [19] A. K. Vyas and F. A. Tobagi. Impact of Interference on the Throughput of a Multihop Path in a Wireless Network. In *IEEE Broadnets*, 2006.